To appear in Experimental Mechanics

SIMULTANEOUS TRANSIENT TEMPERATURE SENSING OF IMPACTED POLYMERS USING INFRARED DETECTORS AND THERMOCOUPLES

A. Regev and D. Rittel(*)
Faculty of Mechanical Engineering
Technion
32000 Haifa, Israel

ABSTRACT

Infrared detectors are probably the most popular device used for transient temperature monitoring of materials deformed in the high strain-rate regime. Embedded thermocouples have also been shown to be suitable for that purpose, especially with poor thermal conductors such as polymers (Rittel, 1998b). However, there is no direct comparison between these two techniques. This paper presents experiments during which commercial polycarbonate specimens were deformed dynamically, while the surface and core temperatures were monitored using an infrared detector and embedded thermocouple respectively. An excellent agreement was obtained between the two techniques, confirming the suitability of thermocouples for transient temperature sensing.

Keywords: infrared, embedded thermocouple, polymer

(*) Corresponding author: merittel@technion.ac.il

INTRODUCTION

Transient temperature sensing (in solids) is a necessity for a number of applications ranging such as high speed machining, high-rate impact and adiabatic shear failure. A thorough review of the experimental techniques can be found in Walley et al. (2000), where it appears that these techniques can broadly be classified into contact and non-contact techniques. The first category includes thermocouples, liquid crystal films, or other heat sensitive coatings, while the latter comprises essentially radiation detection techniques, the most popular being infrared (IR). For large integration times, IR cameras are largely used (Chrysochoos and Louche, 2000), while for faster events one uses IR detectors (Hartley, et al., 1987). As with each experimental method, one needs to tailor the technique to the specific application and required accuracy, so that the IR detector can be a single element (Macdougall and Harding, 1999), or an array for full field imaging (Marchand and Duffy, 1988). Thermocouples have long been used for transient temperature sensing using an analytical approach (Bloomquist and Sheffield, 1980), and sometimes on a more intuitive basis. Rabin and Rittel modeled the transient heat transfer process in a thermocouple (Rabin and Rittel, 1999), showing that when the thermal conductivity contrast between the sensing bead and its surroundings is high, the transient response of the thermocouple is indeed sufficient to capture temperature with a temporal resolution of the microsecond. This is particularly true of polymers into which a small thermocouple can be embedded, such as impacted disks (Rittel, 1999), or the vicinity of crack-tips (Rittel, 1998a).

The two mentioned techniques are essentially different, in the sense that the thermocouple is usually embedded at the *center* of the specimen, whereas the IR detector senses radiation that is emitted from the *surface* of the specimen. Rabin and Rittel (2000) provided guidelines to estimate the error involved in sensing the surface temperature to assess the core temperature, as a function of the specimen dimensions, material properties and time scale. This result was expressed as the relationship between Biot (Bi) and Fourier (Fo) numbers, defined as:

$$\mathrm{Bi} = \frac{\bar{h} \cdot R}{k} \qquad \mathrm{Fo} = \frac{\hat{\alpha} t}{R^2} \qquad (1)$$

where $\bar{h}$ is the combined heat transfer coefficient by convection and radiation, k is the thermal conductivity and R is a characteristic specimen dimension. In addition, $\hat{\alpha}$ and t stand for the thermal diffusivity and time respectively.

These authors got to the conclusion that for polymeric specimens, the difference between the core and the surface temperature should be minimal over these short time scales that are characteristic of high rate impacts. This result is of course quite interesting, would it only be for the ease of use and low cost of thermocouples when compared with infrared detectors' systems.

However, as of today, there has not been a direct experimental comparison of simultaneous temperature sensing using both thermocouples and IR detectors. Such a comparison is required to validate the use (and response) of the embedded thermocouple and its prediction with respect to an IR system.

This paper reports experimental results on this comparison, and the main conclusion is that the proposed analytical solutions are essentially verified experimentally, namely that for small polymeric specimens, the temperature gradient over short time scales is very small so that the embedded thermocouple and IR detector measure the same temperature.

EXPERIMENTAL

a. Specimen, embedded thermocouples (ETC) and loading system

T-type thermocouples, with a wire diameter of 0.125 mm, were embedded to the core of cylindrical specimen made of commercial polycarbonate. The embedding process consisted of drilling a 0.8 mm diameter channel to the specimen's center, inserting one thermocouple and sealing it with home-made dissolved PC chips. The ETC and its glue were allowed to cure at room temperature for at least 24 hours prior to testing. An embedded thermocouple is represented schematically in Figure 1. The cylindrical specimens were loaded by means of a standard Kolsky apparatus (Kolsky, 1949), for which the striker's velocity was systematically varied to produce a range of strain-rates.

b. Infrared system

The detector is a liquid N2 cooled photovoltaic HgCdTe (MCT) array, made by Fermionics (USA). The array forms a vector of 8 pixels, each 45μm×45μm in size, with a center to center pitch of 50μm. The field of view of the detector is 60°, and the wavelength is 6.5μm-12.5μm. The bandbpass of the detector is very large, of the order of several tens of megahertz, but the sampling rate is limited to 5 MHz by the preamplifier (Fermionics, custom made). The sampling

rate was fixed to 2MHz to match the transient mechanical signal. Throughout the experiments, we used one (and always the same) detector only, as this was deemed to provide sufficient results, without having to deal with the array and possible cross-talk issues between the pixels. The detector is focused on the specimen by means of a double Schwartzchild objective (Figure 2) with an equivalent lens of diameter 124 mm, F#=0.65. The resulting magnification of the optics was 1:1.

In a typical experiment, the cylindrical polycarbonate specimen is sandwiched between the bars, and the infrared system, thermocouple and the (incident/reflected) strain gauges are all triggered simultaneously.

The typical temperature resolution of the thermocouple and the IR system is of the order of 0.1K. However, the measured overall background noise of the system is typically of ±3K.

RESULTS

a. Preliminary experiments

Calibration

The most important part of the whole experimental process is the calibration of the system. This is an essential stage for future data processing of each experiment. In this process, the infrared detector and the embedded thermocouple are being calibrated against each other, so that the detector's voltage can be directly converted into a temperature.

The specimen with an ETC is positioned between the bars, facing the IR system in a way that mimics the real test. The polycarbonate specimen is then heated to about 100°C using a hot air blower. Heating is stopped at that stage and the output signals of the IR detector and the thermocouple are simultaneously recorded during the cooling phase. A typical heating phase lasts for about 3 minutes (or less) followed by a cooling phase of maximum 5 minutes, after which the specimen's temperature does not vary noticeably. The signal recorded on the TC is converted into the specimen's core temperature, which is plotted as a function of the IR detector's signal.

One should note that the duration time of the calibration (minutes) and of the experiment (microseconds) are quite different. It is therefore essential to assess that the core and surface temperature are both identical during the calibration phase, to validate the established calibration. Both Biot and Fourier numbers were calculated for a typical calibration and specimen size, as

shown in the sequel, and it was found that the surface and core temperature are quite similar, according to Rabin and Rittel's estimate (2000). Figure 3 shows a typical calibration curve. The key issue for the calibration process is repeatability, so that several calibration curves were produced before each and every new experiment to increase reliability.

Focus and depth of field

The IR system is an optical system that is focused on the specimen's surface. Upon axial compression, the specimen experiences radial expansion, from an initial 10 mm diameter up to typically 14 mm. The radial motion causes a loss of focus of the optical system. However, contrary to an imaging system for which motion of the object's surface can cause blurring of the image, the radiometric system collects energy, so that the motion of a flat homogenous surface should not affect the heat flux. Consequently, the same energy is collected on the detectors' plane, as illustrated in Figure 4. The irradiance H (radiation power) is written as (Smith, 2000):

$$H = T_s \cdot \pi \cdot N \cdot \sin^2 \theta \qquad (1)$$

Where T_s is the system transmission, $N[Watt \cdot ster^{-1} \cdot cm^{-2}]$ is the object's radiance, and θ is the half angle subtended by the exit pupil of the optical system from the image.

The radiance does not change for the motion of a *flat* surface, however, the new circle is located on a *cylindrical* surface and it must be checked whether the cylindrical surface has an additional influence on the radiation which reaches the optical system.

During the experiments, the cylindrical specimens expand diametrically by about 4mm, so that the radiating surface moves 2mm towards the optical system. As shown in Figure 5, this corresponds to an initial point on the original specimen's surface being mapped into a circle with a diameter of about 1.6mm.

The radiation angle at the extreme circle, θ_S, is calculated, as shown in Figure 6, according to:

$$\sin \theta_S = \frac{0.77}{7} \Rightarrow \theta_S = 6.3° \quad (2)$$

Then, Lambert's law is written as (Smith, 2000):

$$J_\theta = J_0 \cos \theta_S \qquad (3)$$

Where J_θ is the intensity of small incremental area at the angle θ_S, J_0 is the intensity at angle 0 and θ_S is the radiation angle. Inserting a typical value of 6.3º for θ_S into eqn. (3), it is found that J_θ decreases to $J_\theta = 0.994 J_0$, which is almost insignificant. This estimation also illustrates the point of the conservation of the radiated energy without the need to account for the de-focusing caused by the specimen's radial expansion.

This estimation was verified with the following procedure. For every set of calibration tests, 10 measurements were made, 5 of which at the exact focus position, and the other 5 at a shifted position, namely at 2mm towards the detector. As shown in Figure 7, these preliminary experiments showed no noticeable change in the measured radiation power, thus validating the above analysis.

b. Experimental results

The cylindrical specimens were prepared from a commercial 10 mm diameter polycarbonate rod, with a height of 3, 4 and 5 mm, respectively. A T-type thermocouple was embedded at the center of each specimen, using the above mentioned technique.

The overall number of experiments exceeds 100, out of which some 20% can be considered as successful, due to early thermocouple tearing, lack of triggering of the system and failure of one of the components of the quite delicate setup. The following experiments are representative, and were carried out at 3 different strain rates, namely $\dot{\varepsilon} = 3000, 6000 \; and \; 8000\, s^{-1}$. Figure 8 shows typical stress-strain-temperature plots for these strain-rates. The temperature is measured simultaneously by the thermocouple and the IR system. A first observation is that the thermocouple and the IR system measure a very similar evolution of the temperature, for strain rates of $\dot{\varepsilon} = 3000 \; and \; 6000 \; s^{-1}$. For the highest strain-rate, $\dot{\varepsilon} = 8000 s^{-1}$, the thermocouple and IR readings are very similar until $\varepsilon \approx 0.5$, beyond which they diverge. Namely, the thermocouple's signal keeps increasing while the IR is decreasing rapidly. Here, one should keep in mind that whereas the thermocouple is attached to the specimen, the latter moves in front of the detector. Another additional factor may cause a decrease in the IR measurement, namely the amount of radiation sensed by the detector.

The collected radiation depends mostly on the optic system and especially on the field of view (FOV). There a difference in the FOV before and after the dynamic test in that the optical

adjustments are suitable as long as the specimen has not significantly deformed such as to alter the FOV. As shown in eqn. (3), the optical angle (system's performance) is calculated as :

$$\alpha_{op} = 2 \cdot \tan^{-1}\left(\frac{D/2}{S}\right) \approx 42^{\circ} \quad (3)$$

Were α_{op} is the system's performance according to the system's dimensions, D (124mm) is the aperture, and S (162mm) is the specimen's position as shown in Figure 9(A).

After significant deformation, or for a thin specimen, the angle limitation with the thin specimen is 37°, as given by :

$$\beta_{op} = 2 \cdot \tan^{-1}\left(\frac{t_s}{d_B - d_S}\right) \approx 37^{\circ} \quad (4)$$

Were β_{op} is the limiting angle according to the new system's dimensions, d_B (19.05mm) is the bar diameter, d_S (10mm) is the specimen diameter and t_s (3mm) is the specimen's thickness as shown in Figure 9(B). This means that that the FOV is partially blocked for 3mm or less thick specimens.

DISCUSSION and CONCLUSIONS

Transient temperature measurements were carried out simultaneously using an infrared system and an embedded thermocouple in a dynamically loaded ductile polymer.

The measured signals were converted into temperature, based upon the premise that the core and the surface temperatures of the specimen were identical during the calibration procedure. To verify this point, on the characteristic Fourier and Biot numbers were calculated as:

$$\mathrm{Bi} = \frac{\bar{h} \cdot R}{k} = \frac{4.33 \cdot (5 \div 7) 10^{-3}}{0.29} = 0.07 \div 0.1$$

$$\mathrm{Fo} = \frac{\hat{\alpha} \cdot t}{R^2} = \frac{1.9 \cdot 10^{-7} \cdot 180}{\left((5 \div 7) \cdot 10^{-3}\right)^2} = 0.57 \div 0.29$$

Where the combined heat transfer coefficient by convection and radiation $\bar{h} = 4.33\left[W/m^2 \cdot K\right]$, the thermal conductivity $k = 0.29\left[W/m \cdot K\right]$, the thermal diffusivity $\hat{\alpha} = 1.9 \cdot 10^{-7}\left[m^2/s\right]$

(Lienhard and Lienhard, 2003), the cylinder radius $R = 5 \cdot 10^{-3} \div 7 \cdot 10^{-3} [\mathrm{m}]$. The typical time scale is assumed to be $t = 180 [\mathrm{sec}]$.

These points can be inserted into the graphic solution of Rabin and Rittel (2000) for the difference of temperatures between the core and the surface of the specimen. As shown in Figure 10, the temperature difference is relatively small, and in any case remains inferior to 10%. Consequently, this estimation shows that during the calibration procedure, the core and the surface temperatures differ by less than 10%, which for all practical purposes amounts to considering them as very close one to the other. Having validated the basic assumption underlying the calibration process, it can also be noted that for an impact experiment, the time duration is some 4 orders of magnitude shorter so that here too, the core and surface temperatures are expected to be very similar. This is precisely what is observed at the various strain rates investigated in this work, as shown in Figure 8, irrespective of the strain-rate. This study therefore confirms that thermocouples provide an accurate indication of the transient temperature changes in the impacted polymeric specimens, in perfect agreement with previous work (Bloomquist and Sheffield, 1980; Rittel, 1998b).

Concerning the infrared setup, this study revealed various factors that influence the radiation power from the specimen. While de-focussing due to specimen radial motion does not cause large variations in the measured radiated power, variations of the field of view are seen to severely limit the measurements of the surface temperature. Indeed, the field of view decreases as the specimen is being compressed longitudinally up to a point where the steel bars prevent the radiation from reaching the specimen (Figure 9(C)). The thermocouple does not suffer from the same limitations so that a practical conclusion is to use *both* thermocouples and infrared detectors whenever possible.

To summarize the main outcome of this study in a graphical way, the temperature measured with the IR system is plotted in Figure 11 as a function of that determined from the embedded TC, for several typical experiments. The results are all noted to align close to the 45º line, indicating aas mentioned the excellent agreement between the two measurement techniques.

To conclude:

- This study has shown that the embedded thermocouple technique can provide a precise measurement of transient temperature changes of dynamically loaded polymers.
- The results support the previous analytical results of Rabin and Rittel (2000).

Acknowledgement

The Reviewer is acknowledged for suggesting the inclusion of Figure 11.

FIGURES

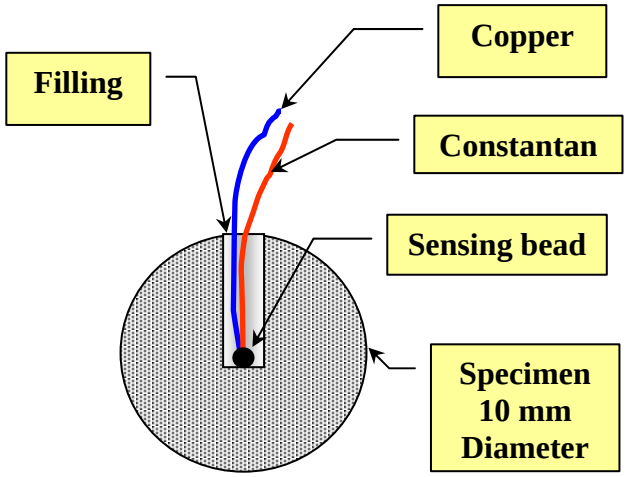

Figure 1: Schematic representation of an embedded thermocouple.

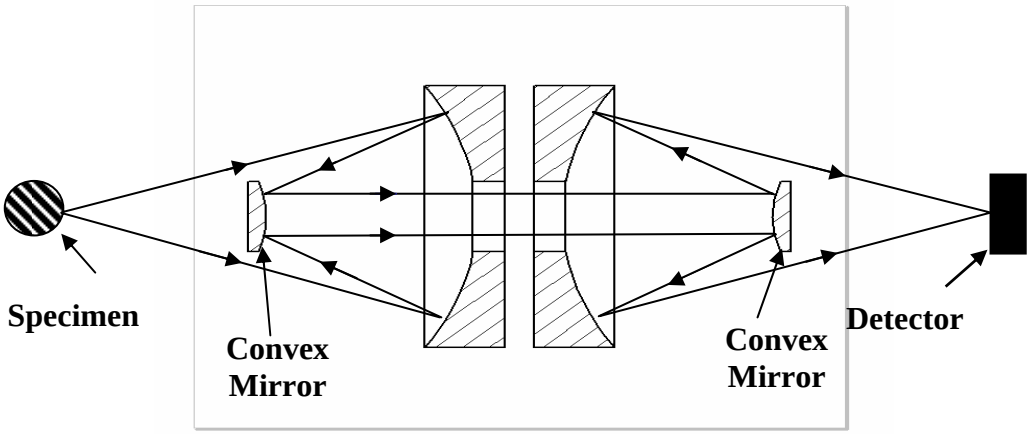

Figure 2: Schematic representation of the optical system.

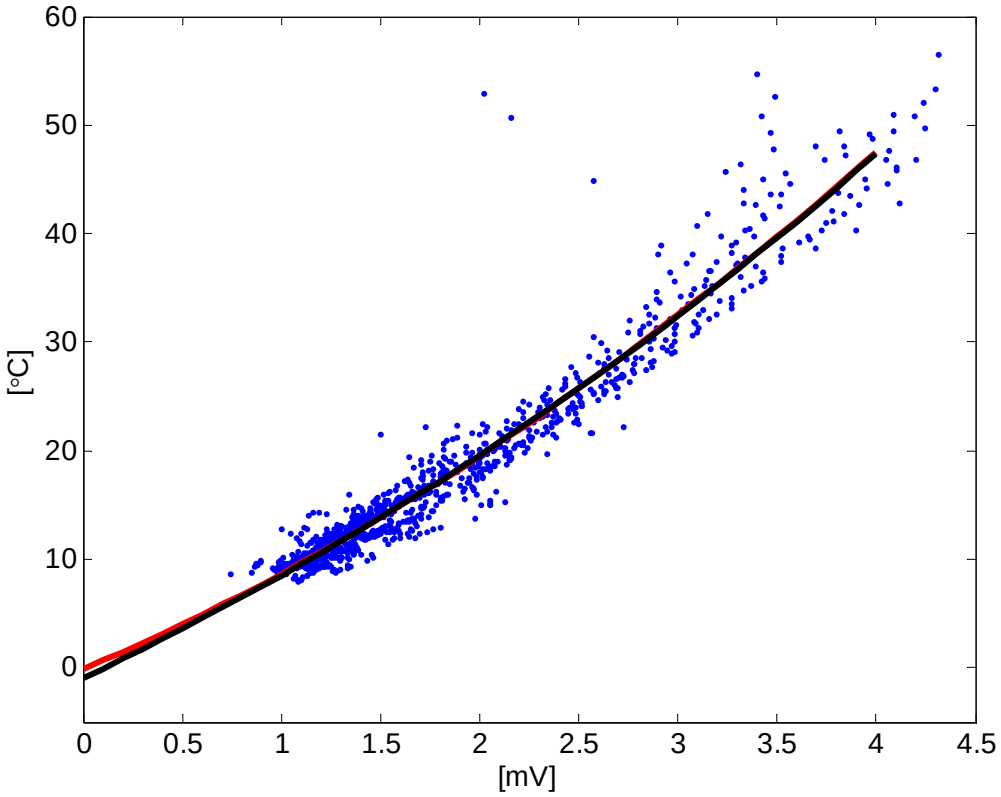

Figure 3: A typical calibration curve converting the IR output voltage into temperature rise. The two solid lines correspond to polynomial and exponential curve fitting.

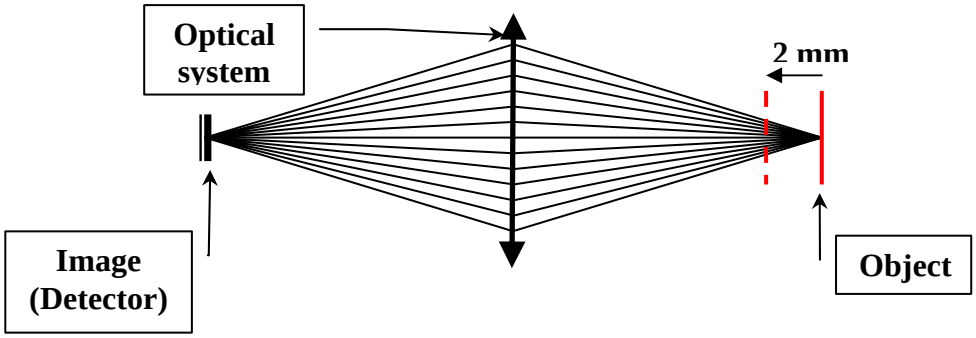

Figure 4: Schematic representation of the flow of energy into the detector. Note that the same energy is detected, irrespective of the actual focus.

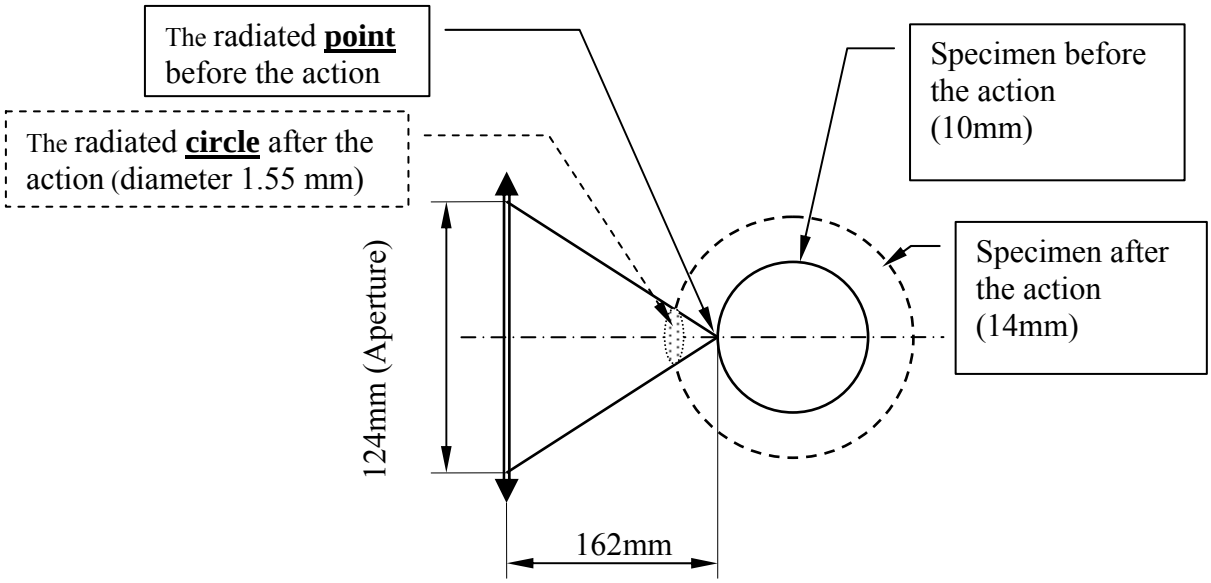

Figure 5: Movement of the specimen surface and creation of the radiated circle.

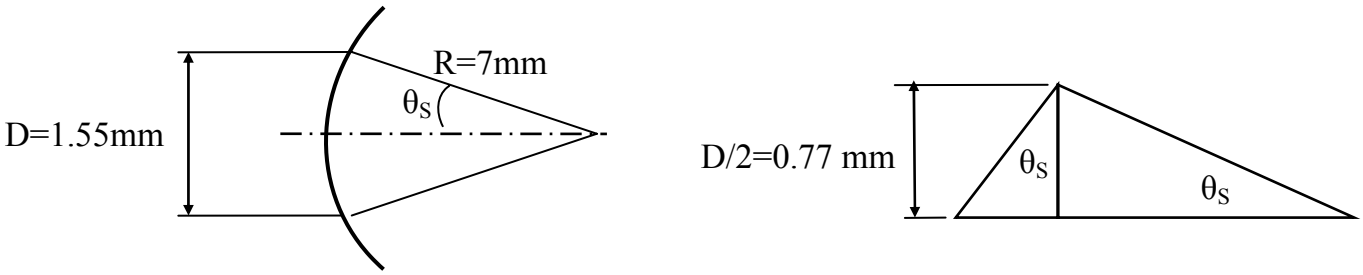

Figure 6: The largest angle on the radiated circle (specimen diameter – 14mm)

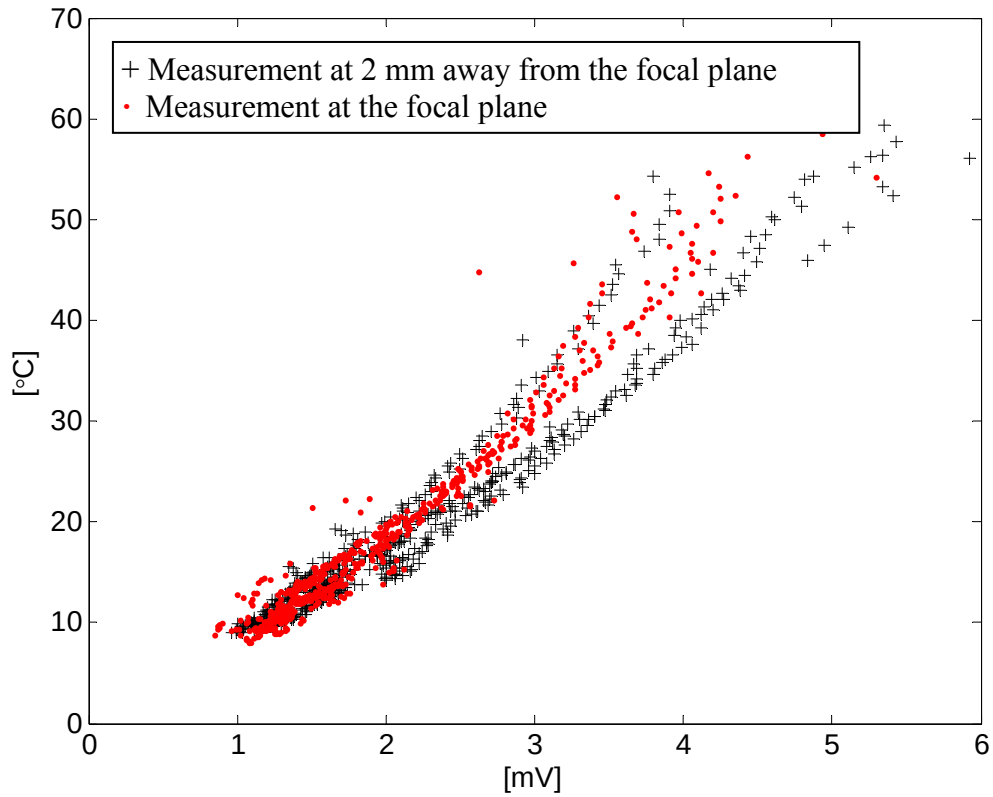

Figure 7: Typical calibration test results: '+' indicates measurement at the focal plane and '·' stands for measurement at 2 mm away from the focal plane. Within statistical fluctuations, the results are similar, indicating that the energy reaching the detector is conserved.

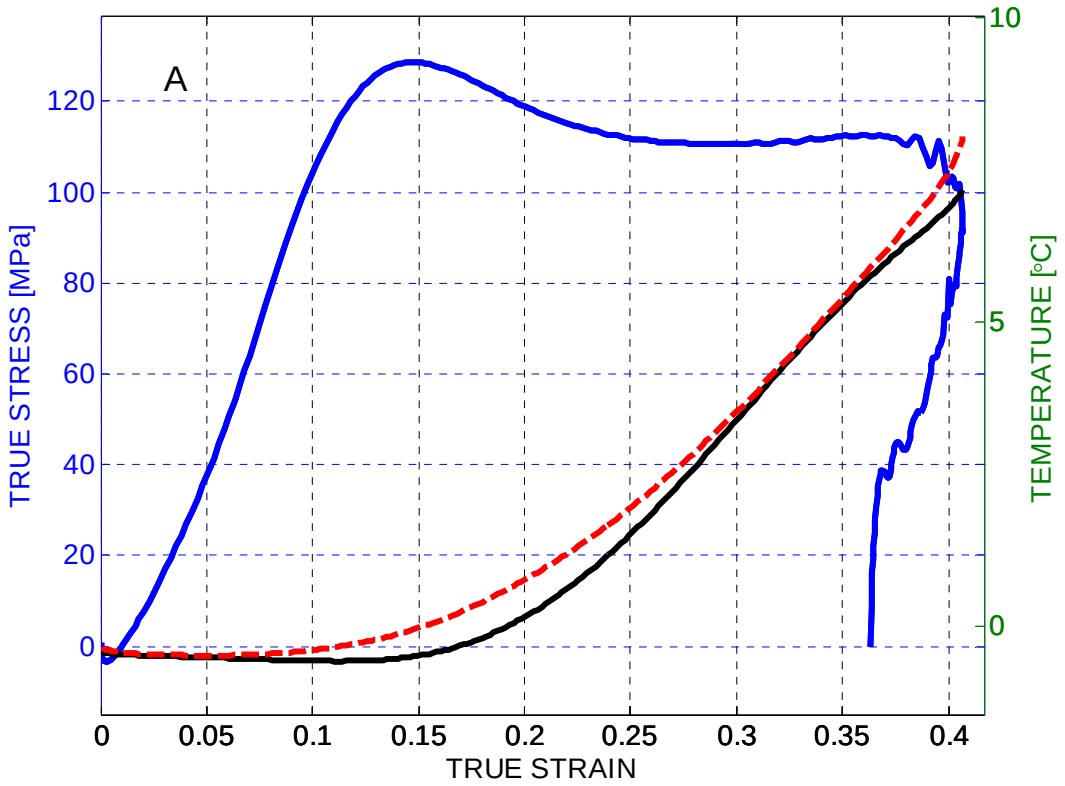

Figure 8 (A): Typical stress-strain-temperature plot at $\dot{\varepsilon} = 3000\,\mathrm{s}^{-1}$. The solid temperature line indicates the thermocouple and the dashed one indicates IR reading. Note the high similarity between TC and IR readings. Compressive stresses and strains are plotted as positive.

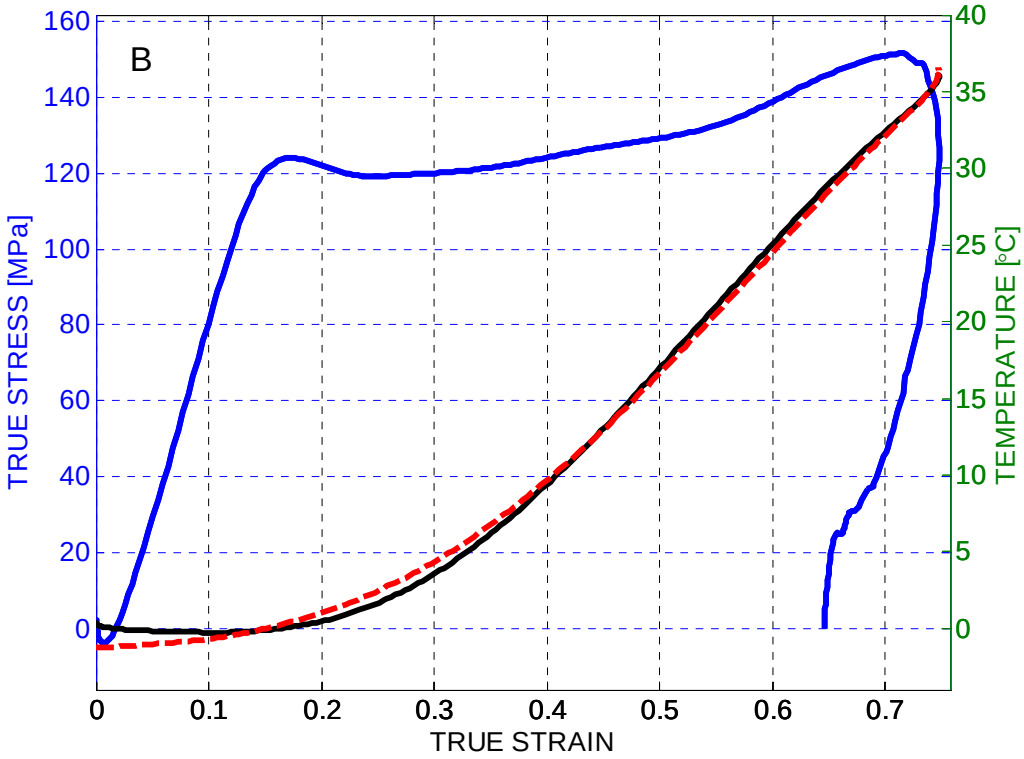

Figure 8 (B): Typical stress-strain-temperature plot at $\dot{\varepsilon} = 6000\,\mathrm{s}^{-1}$. The solid temperature line indicates the thermocouple and the dashed one indicates IR reading. Note the high similarity between TC and IR readings. Compressive stresses and strains are plotted as positive.

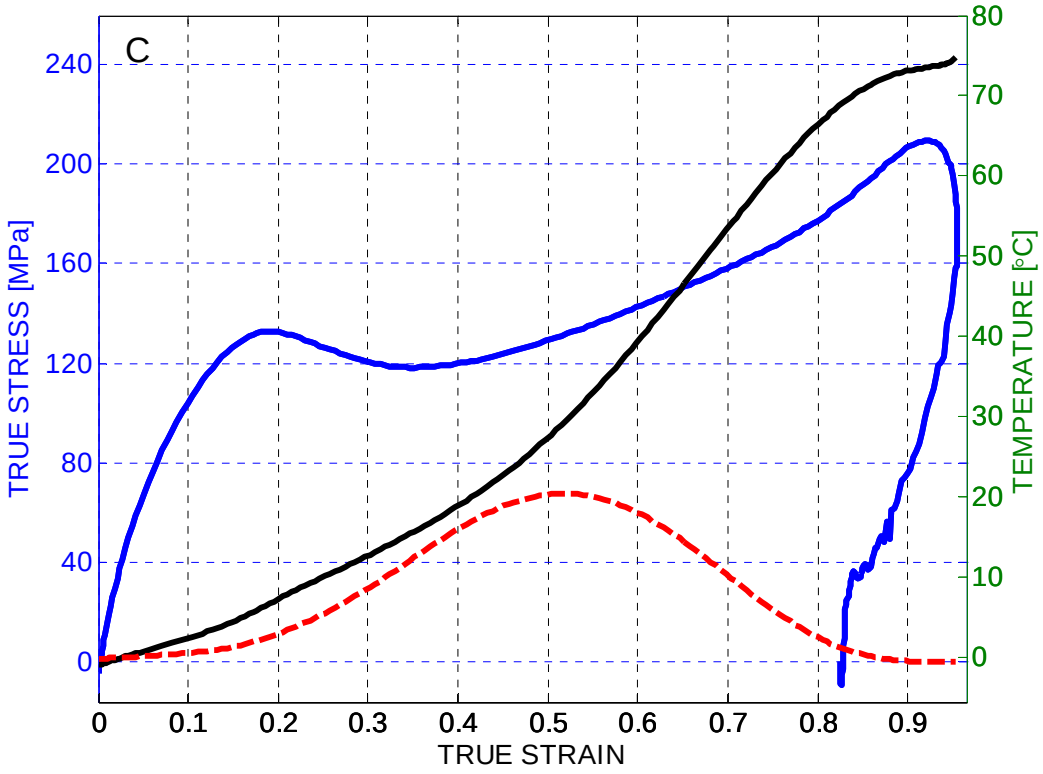

Figure 8 (C): Typical stress-strain-temperature plot at $\dot{\varepsilon} = 8000\,\mathrm{s}^{-1}$. The solid temperature line indicates the thermocouple and the dashed one indicates IR reading. Note the high similarity between TC and IR readings until $\varepsilon \approx 0.5$. Past that point, the field of view of the IR system is hidden by the steel bars. Compressive stresses and strains are plotted as positive.

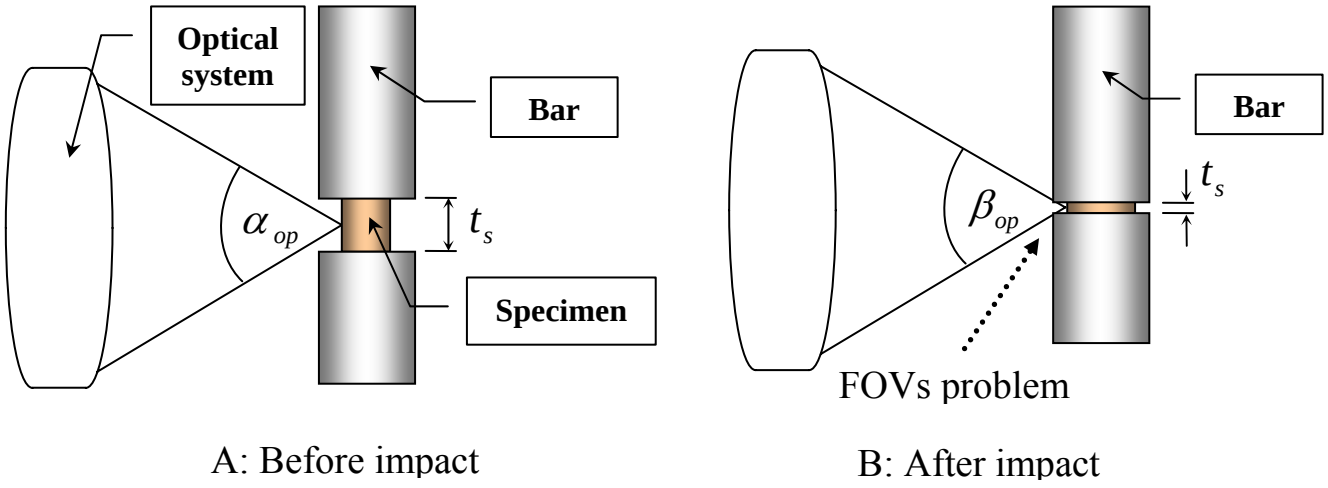

Figure 9: Reduction of the field of view (A) as a result of the specimen's shortening during the test (B).

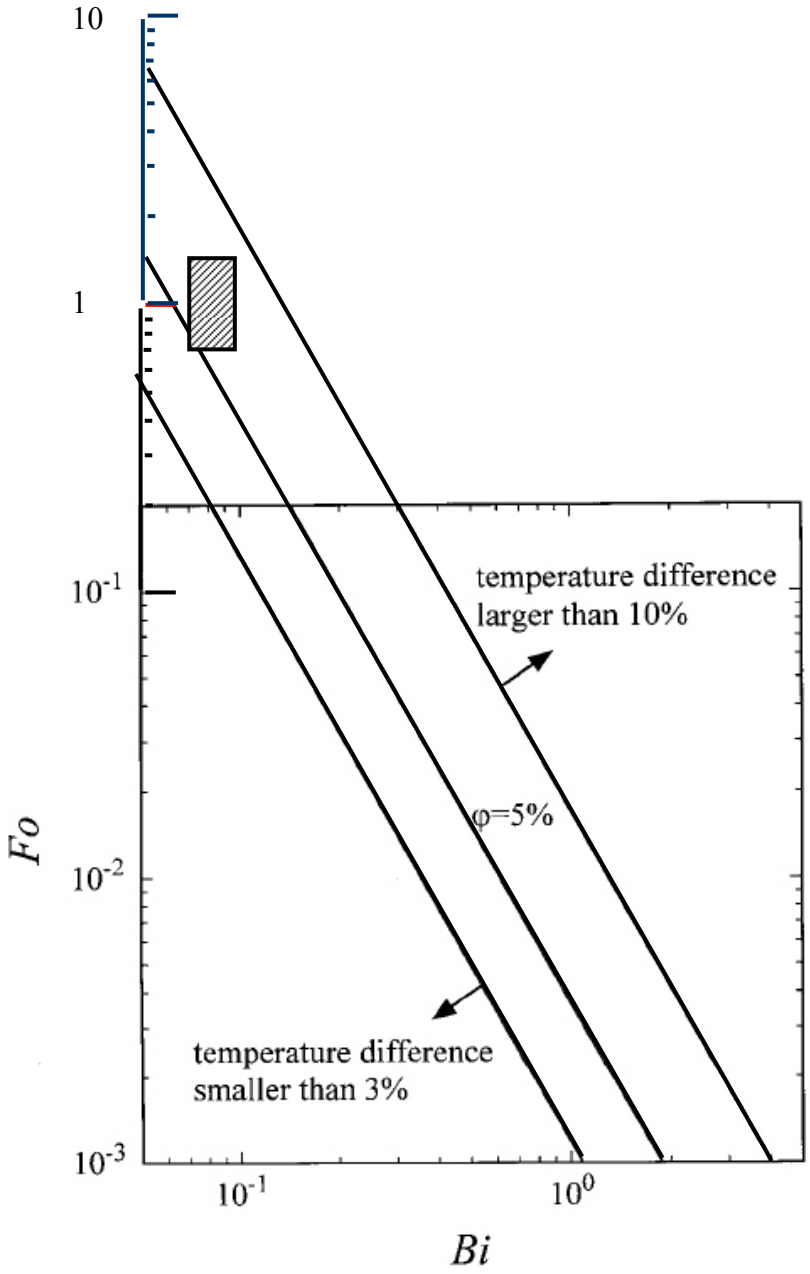

Figure 10 : Core to surface temperature difference, as a function of Fo vs. Bi curves, reprinted from Rabin and Rittel (2000). The time scale (Fo) has been extrapolated to include longer time scales that are characteristic of the calibration procedure, for which the specimen is heated during some 180 s (or less). The hatched rectangle covers the range of Fo and Bi characteristic to the calibration procedure. It can be noted that the maximum temperature difference between the core and the surface of the specimen remains always inferior to 10%.

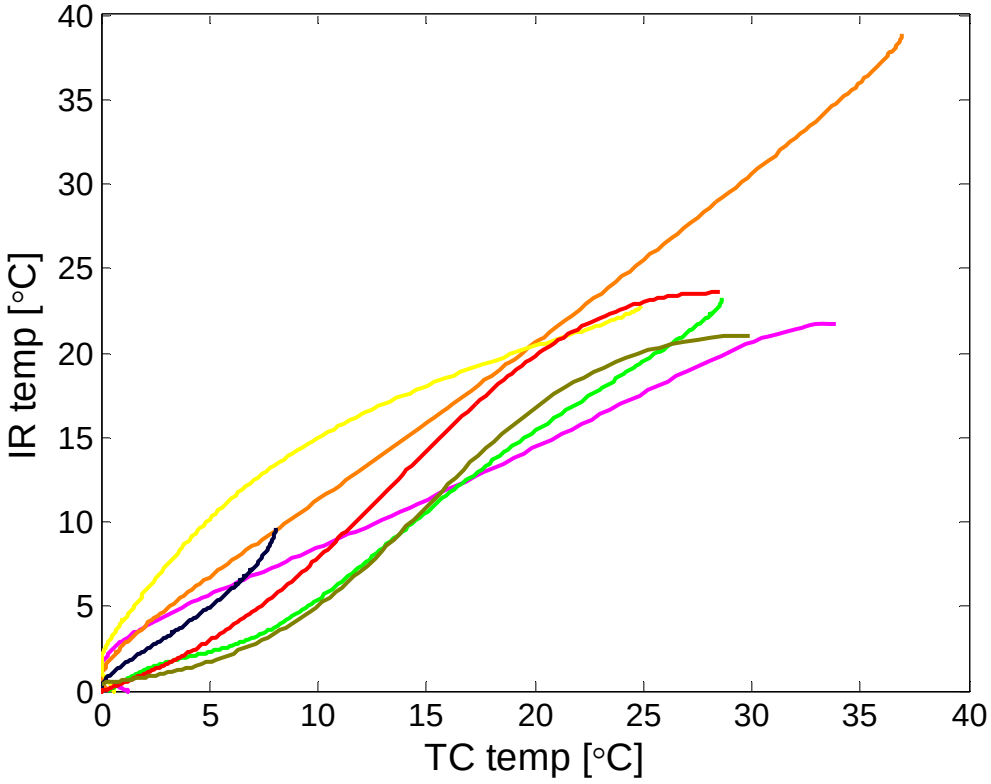

Figure 11: Plot of the temperature rise measured with the IR system as a function of that determined from the embedded TC, for several typical tests. Note the very good correspondence between the two.

REFERENCES

Bloomquist, D.D., Sheffield, S.A., 1980. Thermocouple temperature measurements in shock compressed solids. J. Appl. Phys. 51 (10), 5260-5266.

Chrysochoos, A., Louche, H., 2000. An infrared image processing to analyse the calorific effects accompanying strain localisation. Int. J. Engng. Sc. 38 (16), 1759-1788.

Hartley, K.A., Duffy, J., Hawley, R.H., 1987. Measurement of the temperature profile during shear band formation in mild steels deforming at high-strain rates. J. Mech. Phys. Solids 35 (3), 283-301.

Kolsky, H., 1949. An investigation of the mechanical properties of materials at very high rates of loading. Proc. Phys. Soc. London 62-B, 676-700.

Lienhard, J.H.I.V., Lienhard, J.H.V., 2003. A heat transfer textbook. Phlogiston Press, Lexington MA.

Macdougall, D.A.S., Harding, J., 1999. A constitutive relation and failure criterion for Ti6A14V alloy at impact rates of strain J. Mech. Phys. Solids 47 (5), 1157-1185.

Marchand, A., Duffy, J., 1988. An experimental study of the formation process of adiabatic shear bands in a structural steel. J. Mech. Phys. Solids 36 (3), 251-283.

Rabin, Y., Rittel, D., 1999. A model for the time response of solid-embedded thermocouples. Experimental Mechanics 39 (1), 132-136.

Rabin, Y., Rittel, D., 2000. Infrared temperature sensing of mechanically loaded specimens: thermal analysis. Experimental Mechanics 40 (2), 197-202.

Rittel, D., 1998a. Experimental investigation of transient thermoelastic effects in dynamic fracture. International Journal of Solids and Structures 35 (22), 2959-2973.

Rittel, D., 1998b. Transient temperature measurement using embedded thermocouples. Experimental Mechanics 38 (2), 73-79.

Rittel, D., 1999. On the conversion of plastic work to heat during high strain rate deformation of glassy polymers. Mechanics of Materials 31 (2), 131-139.

Smith, W.J., 2000. Modern optical engineering. McGraw and Hill, New York, NY.

Walley, S.M., Proud, W.G., Rae, P.J., Field, J.E., 2000. Comparison of two methods of measuring the rapid temperature rises in split Hopkinson bar specimens. Rev. Sc. Instr. 71 (4), 1766-1771.